DOI: 10.1002/ejic.201100140

Formation of Chiral Heteronuclear Ln^{III} Assemblies by Ion Pair Formation

Janusz Gregoliński,[a] Robert Wieczorek,[a] and Jerzy Lisowski*[a]

Keywords: Ion pairs / Lanthanides / Macrocyclic ligands / Supramolecular chemistry / Pfeiffer effect

Cationic Ln^{III} complexes with the chiral macrocycle L, (P)-[LnL$_{RRRRRR}$]$^{3+}$, interact with anionic Ln^{III} tris(dipicolinate) complexes, [Ln′(dpa)$_3$]$^{3–}$, forming tight hydrogen-bonded ion pairs in solution. Formation of these pairs has been documented by the DFT calculations, and a strong paramagnetic shift of the signals of the diamagnetic cation interacting with the paramagnetic anion was observed. This ion pair interaction leads to spectral enantiodifferentiation of the Λ-[Ln′(dpa)$_3$]$^{3–}$ and Δ-[Ln′(dpa)$_3$]$^{3–}$ enantiomers of the anionic complex. Although no Pfeiffer effect was observed for the (P)-[LnL$_{RRRRRR}$]$^{3+}$ diastereomers of the cationic complex, the (M)-[LnL$_{RRRRRR}$]$^{3+}$ diastereomers induce CD signals in the anionic [Ln′(dpa)$_3$]$^{3–}$ partner. These spectra indicate a Pfeiffer effect, i.e. a shift of equilibrium between the Λ-[Ln′(dpa)$_3$]$^{3–}$ and Δ-[Ln′(dpa)$_3$]$^{3–}$ enantiomers. This effect arises from the ion pair interaction between the anionic complex [Ln′(dpa)$_3$]$^{3–}$ and the intact cationic complex as well as between [Ln′(dpa)$_3$]$^{3–}$ and L. The protonated macrocycle (H$_3$L$_{RRRRRR}$)$^{3+}$ forms highly insoluble salts with [Ln′(dpa)$_3$]$^{3–}$. These supramolecular compounds are formed by the reaction of L, acids and [Ln′(dpa)$_3$]$^{3–}$ anions. The same product can also be formed by the reaction of (M)-[LnL$_{RRRRRR}$]$^{3+}$ with three equivalents of dipicolinic acid. The model structure of (H$_3$L$_{RRRRRR}$)[Ln′(dpa)$_3$] corresponds with a linear polymer with alternate cationic macrocycles and anionic [Ln′(dpa)$_3$]$^{3–}$ complexes interacting through charge interactions and multiple hydrogen bonds.

Introduction

The formation of ion pairs in solution is an important chemical and biological phenomenon.[1] This process plays a role in medical applications of ionic metal complexes. The interaction between paramagnetic anionic thulium(III) complexes such as TmDOTP$^{5–}$ and Na$^+$ cations has been used for monitoring the concentration of sodium in intact tissues using NMR imaging. In this application, the paramagnetic complex acts as a shift reagent that forms ion pairs with extracellular Na$^+$. This ion pairing induces a frequency shift in the ^{23}Na NMR signal of the paired ion that is separate from that of the intracellular Na$^+$. Ion pairing interactions between [Co(en)$_3$]$^{3+}$ and TmDOTP$^{5–}$ have been studied in the context of new formulations of such ^{23}Na NMR shift reagents with lower osmolality.[2] Similarly, the formation of ion pairs between cationic and anionic lanthanide(III) complexes has been studied as part of the search for more efficacious Gd^{III}-based contrast agents for magnetic resonance imaging.[3] In the case of chiral anions and cations, an asymmetric interaction can sometimes lead to chiral recognition during ion pair formation, which can be utilised for the detection of enantiomers as well as asymmetric resolution, induction and synthesis.[4] Formation of ion pairs involving chiral partners may play an important role in catalysis. For instance, the interaction of chiral tetraaminophosphonium cations with phosphite anions has been used in asymmetric hydrophosphonylation of aldehydes.[5] The same cations together with phenoxide anions build a supramolecular catalyst based on ion pairing and hydrogen bonds that catalyze the stereoselective conjugate addition of acyl anion equivalents to α, β-unsaturated ester surrogates.[6]

Here we present the formation of heteronuclear lanthanide(III) supramolecular assemblies of anionic lanthanide(III) tris(dipicolinate) [tris(2,6-pyridinedicarboxylate)] complexes, [Ln′(dpa)$_3$]$^{3–}$, and the cationic complexes [LnL]$^{3+}$ of a chiral macrocycle L (Scheme 1). The latter complexes are chiral, with L wrapped around the Ln^{III} ion in a helical fashion.[7,8] These assemblies can be isolated as four pure stereoisomers corresponding to the two enantio-

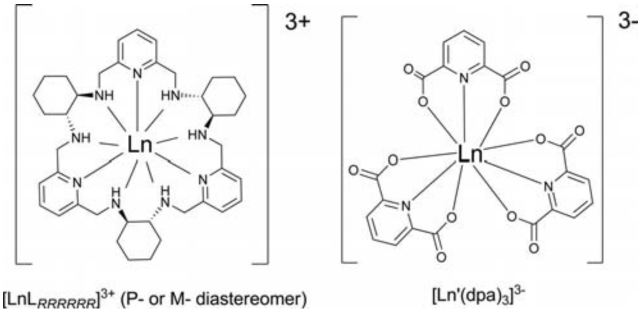

Scheme 1. The cationic complex [LnL]$^{3+}$ and the anionic complex [Ln′(dpa)$_3$]$^{3–}$.

---

[a] Department of Chemistry, University of Wrocław,
14 F. Joliot-Curie, 50-383 Wrocław, Poland
Fax: +48-71-3282348
E-mail: jurekl@wchuwr.pl

Supporting information for this article is available on the WWW under http://dx.doi.org/10.1002/ejic.201100140.

meric pairs of the (*P*)-[LnL$_{RRRRRR}$]$^{3+}$/(*M*)-[LnL$_{SSSSSS}$]$^{3+}$ diastereomer and the (*M*)-[LnL$_{RRRRRR}$]$^{3+}$/(*P*)-[LnL$_{SSSSSS}$]$^{3+}$ diastereomer. The two diastereomeric forms differ in the direction of the helical twist of the macrocycle. The nine-coordinate, tris(terdentate), propeller-shaped [Ln′(dpa)$_3$]$^{3–}$ complexes are of D_3 symmetry and exist in solution as a labile racemic mixture of Λ and Δ enantiomers.[9] These complexes have been studied as luminescent[10] and NMR[11] spectroscopic probes and as nonlinear optical materials.[12] [Ln′(dpa)$_3$]$^{3–}$ complexes have also been used in protein crystallography to facilitate crystallization and solution of crystal structures.[13] This latter application is related to the formation of a hydrogen-bonded ion pair between this anionic complex and the ethylguanidine cation.

We are interested in the observation of the Pfeiffer effect in the interaction of chiral, enantiopure cationic Ln^{III} complexes and chiral, racemic anionic Ln^{III} complexes. The Pfeiffer effect[14] is a shift in the racemic equilibrium of a racemic but kinetically labile metal complex caused by an interaction with a chiral compound. This effect has been studied for racemic propeller-shaped transition metal complexes. The Pfeiffer effect has also been intensively investigated for lanthanide(III) tris(dipicolinate) complexes[15] and related tris(2,2′-oxydiacetate) complexes[16] interacting with chiral agents such as amino acids. Most of these studies were performed by using circularly polarized luminescence and CD spectroscopy. We have generated and characterized heteronuclear pairs of cationic complexes [LnL]$^{3+}$ with the anionic complexes [Ln′(dpa)$_3$]$^{3–}$. It should be noted that the selective formation of heteronuclear f–f′ complexes is difficult due to the similar nature of the Ln^{III} ions.[17] During this study we have also observed the formation of another type of supramolecular assembly, which is a polymeric compound composed of anionic [Ln′(dpa)$_3$]$^{3–}$ complexes and the cationic protonated form of the macrocycle (H$_3$L)$^{3+}$.

Results and Discussion

NMR Studies of Ion-Pair Formation between the (*P*)-[LnL$_{RRRRRR}$]$^{3+}$ Diastereomers and [Ln′(dpa)$_3$]$^{3–}$

In paramagnetic metal complexes the nucleus experiences an additional shift observed in the NMR spectrum called the isotropic shift (δ_{iso}), which arises from the interaction of the nuclear and electronic spins.[18] In the case of lanthanide complexes, this paramagnetic shift is often called the lanthanide induced shift. The isotropic shift can be separated into the through space, dipolar contribution (also called pseudocontact) and the through bonds, contact contribution. For a series of isostructural axial lanthanide(III) complexes, including tris(dipicolinate) complexes, the dipolar shift is proportional to the C_j coefficient and the axial geometric factor $<1 - 3\cos^2\theta/r^3>$ (where the constant C_j depends on the Ln^{III} ion[19] and r and θ are polar coordinates of the given nucleus).

Titration of a D$_2$O solution of the diamagnetic (*P*)-[LuL$_{RRRRRR}$]$^{3+}$ with D$_2$O solutions of the paramagnetic [Ln′(dpa)$_3$]$^{3–}$ results in profound spectral changes (Figure 1 and Figure 2). The signals of the diamagnetic Lu^{III} complex shift gradually with the increasing amount of paramagnetic complex. This effect is particularly strong in the titration with [Dy(dpa)$_3$]$^{3–}$; the signals of the macrocycle move to lower frequency and become very broad (Figure 1). The spectrum obtained after the addition of 1 equiv. of Na$_3$[Dy(dpa)$_3$]·13H$_2$O to (*P*)-[LuL$_{RRRRRR}$](NO$_3$)$_3$·7H$_2$O in D$_2$O/CD$_3$OD, exhibits signals of L with chemical shift values as low as –23.5 ppm and linewidths exceeding 200 Hz. This kind of spectrum is typical for a paramagnetic complex, although it arises from the diamagnetic (*P*)-[LuL$_{RRRRRR}$]$^{3+}$ complex. The protons of L in the diamagnetic Lu^{III} complex clearly experience the influence of the paramagnetic

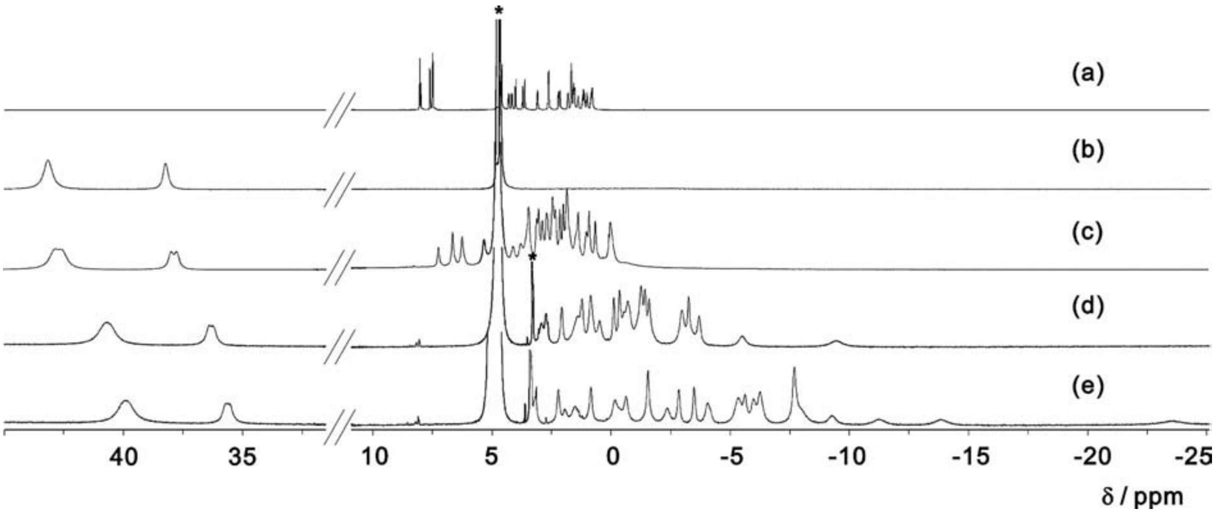

Figure 1. Regions of the ^{1}H NMR spectra (D$_2$O, 298 K) of (a) (*P*)-[LuL$_{RRRRRR}$]$^{3+}$, (b) [Dy(dpa)$_3$]$^{3–}$, (c) (*P*)-[LuL$_{RRRRRR}$]$^{3+}$ after addition of 1 equiv. of [Dy(dpa)$_3$]$^{3–}$, (d) after dilution with CD$_3$OD 1:1 v/v and (e) after further dilution with CD$_3$OD 1:2 v/v. The asterisk denotes the solvent signal.

shift. This shift has to arise from the close proximity of a paramagnetic ion, which in this case is Dy^{III}. The origin of the shifts has to be dipolar, as there is no electronic communication (covalent bond network) between the cationic Lu^{III} complex and the anionic Dy^{III} complex. The appearance of strongly paramagnetically shifted lines of the diamagnetic (P)-$[LuL_{RRRRRR}]^{3+}$ complex is direct evidence of the formation of a tight ion pair between (P)-$[LuL_{RRRRRR}]^{3+}$ and $[Dy(dpa)_3]^{3-}$. Similarly, the signals of (P)-$[LuL_{RRRRRR}]^{3+}$ interacting with $[Yb(dpa)_3]^{3-}$ in D_2O are paramagnetically shifted. This time the shifts are more moderate (Figure 2) with most of the signals shifted to higher frequency.

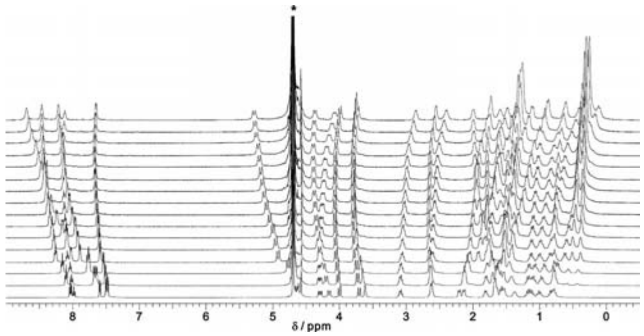

Figure 2. Changes to the ^1H NMR signals of (P)-$[LuL_{RRRRRR}]^{3+}$ (D_2O, 298 K) upon successive addition of 0, 0.05, 0.15, 0.25, 0.35, 0.50, 0.69, 0.91, 1.12, 1.33, 1.54, 1.73, 2.02, 2.50, 3.03 and 3.50 equiv. of paramagnetic $[Yb(dpa)_3]^{3-}$ from bottom to top, respectively. The asterisk indicates the solvent signal, the other two most intense signals in the top spectrum correspond to $[Yb(dpa)_3]^{3-}$ (including the split signal with the smallest chemical shift, corresponding to the *meta* protons of the dipicolinate ligand).

The extent of the paramagnetic shifts experienced by the macrocycle protons in (P)-$[LuL_{RRRRRR}]^{3+}$ is solvent dependent. Successive addition of CD_3OD to D_2O solutions containing (P)-$[LuL_{RRRRRR}]^{3+}$ and $[Ln'(dpa)_3]^{3-}$ results in the substantial increase of paramagnetic shifts (Figure 1, Supporting Information Figure S1). This increase is caused by a shift of equilibrium among the free complex-cation, free complex-anion and the ion pair. The strong enhancement of the paramagnetic shifts caused by the addition of methanol confirms the formation of a supramolecular assembly based on hydrogen-bonded ion pairs, as the less polar methanol favours formation of such assemblies. On the other hand, hydrophobic interactions should be weakened by the addition of methanol and one would expect to observe a decrease of paramagnetic shifts reflecting an equilibrium shift towards dissociation. It follows that the hydrophobic interaction is not a key factor in the assembly of the (P)-$[LnL_{RRRRRR}]^{3+}/[Ln'(dpa)_3]^{3-}$ ion pair.

The substantial dipolar shift values experienced by the protons of the macrocycle do not only indicate the close proximity of the paramagnetic anion, but also the fact that the macrocyclic complex must have a preferred orientation (or orientations) with respect to the anionic complex containing the paramagnetic Ln'^{III} ion. Otherwise, in the case of equal probability of all orientations, the $<1 - 3\cos^2\theta/r^3>$ term would average to zero leading to no paramagnetic shift of the macrocycle signals. It should be noted that nonrandom orientations have been observed previously for ion pair-containing transition metal complexes.[20a,20b]

The opposite signs and relative magnitude of the paramagnetic shifts of the macrocycle protons caused by the interaction of (P)-$[LuL_{RRRRRR}]^{3+}$ with $[Dy(dpa)_3]^{3-}$ or $[Yb(dpa)_3]^{3-}$ are in agreement with the magnetic properties of the Dy^{3+} and Yb^{3+} ions, particularly with the relative C_j values[19] for these ions. The paramagnetic shifts of the macrocyclic protons of (P)-$[LuL_{RRRRRR}]^{3+}$ (moved to lower frequency) induced by the paramagnetic anion $[Dy(dpa)_3]^{3-}$, are of opposite sign to those of the pyridine protons of the $[Dy(dpa)_3]^{3-}$ complex itself (moved to higher frequency). This corresponds to the different orientation of these protons with respect to the cone determined by the $<1 - 3\cos^2\theta/r^3>$ term. For protons with θ angle values of $0 < \theta < 54.7°$, the sign of the dipolar contribution should be opposite to that of protons with θ angle values of $54.7 < \theta < 125.3°$.

Variations in the chemical shifts of the macrocycle seen during the successive addition of $[Ln'(dpa)_3]^{3-}$ to (P)-$[LuL_{RRRRRR}]^{3+}$ are accompanied by splitting and chemical shift variation of the dipicolinate signals of $[Ln'(dpa)_3]^{3-}$. This corresponds to the NMR enantiodifferentiation of the optical isomers of the anionic complex (Figures 1 and 2). The ^1H NMR signals of the *meta*- and *para*-protons of the dipicolinate ligand in the paramagnetic $[Dy(dpa)_3]^{3-}$ and $[Yb(dpa)_3]^{3-}$ complexes are broad singlets (Figure 1, b), which split after addition of (P)-$[LuL_{RRRRRR}]^{3+}$ (Figure 1, c, Figure 2). This splitting reflects the formation of diastereomeric ion pairs (P)-$[LuL_{RRRRRR}]^{3+}/\Lambda$-$[Ln(dpa)_3]^{3-}$ and (P)-$[LuL_{RRRRRR}]^{3+}/\Delta$-$[Ln(dpa)_3]^{3-}$. In contrast, splitting of the macrocyclic resonances is not observed. This behaviour is in agreement with a fast (on the NMR timescale) exchange equilibrium between the ion pair and its constituents and a slow (on the NMR timescale) exchange equilibrium between Λ-$[Ln(dpa)_3]^{3-}$ and Δ-$[Ln(dpa)_3]^{3-}$ (Scheme 2).

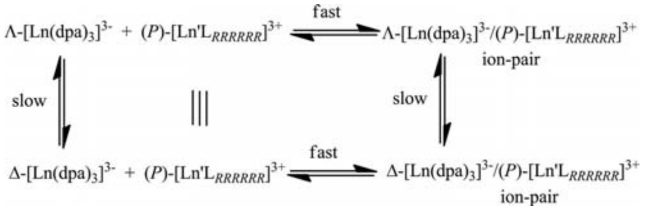

Scheme 2. Exchange in the diastereomeric ion pairs.

Splitting of the dipicolinate ^1H NMR signals was also observed for the pair of diamagnetic complexes (P)-$[LuL_{RRRRRR}]^{3+}$ and $[Lu(dpa)_3]^{3-}$. This effect is presented in Figure 3, and the spectrum shows two doublets and two triplets of the dipicolinate ligand as well as a single set of macrocyclic resonances. In this case the splitting and shift of the dipicolinate signals as well as the shift of the macrocyclic signals arise from aromatic ring current effects and are much smaller than those observed for the paramagnetic Yb^{III} and Dy^{III} analogues. As expected, the spectral changes observed for the (*P*)-[LuL$_{RRRRRR}$]$^{3+}$/[Lu(dpa)$_3$]$^{3-}$ pair are identical to those observed for the (*M*)-[LuL$_{SSSSSS}$]$^{3+}$/[Ln(dpa)$_3$]$^{3-}$ pair containing the other enantiomer of the cationic macrocyclic complex.

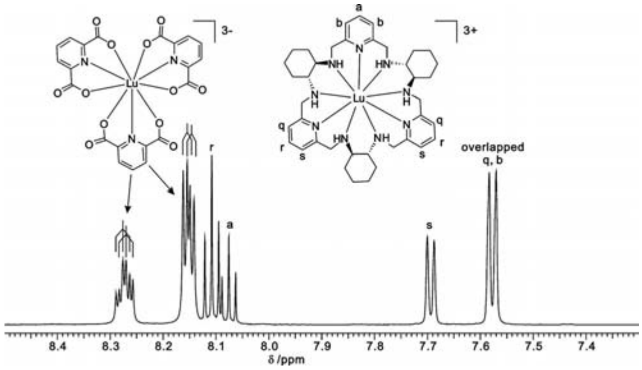

Figure 3. Splitting of the dipicolinate ^{1}H NMR signals of diamagnetic [Lu(dpa)$_3$]$^{3-}$ caused by the addition of diamagnetic (*P*)-[LuL$_{RRRRRR}$]$^{3+}$.

Finally we have titrated paramagnetic (*P*)-[YbL$_{RRRRRR}$]$^{3+}$ with diamagnetic [Lu(dpa)$_3$]$^{3-}$. In this case the shifts and separations of the signals of the dipicolinate complex are larger than those observed for the (*P*)-[LuL$_{RRRRRR}$]$^{3+}$/[Lu(dpa)$_3$]$^{3-}$ pair, whereas the shifts of (*P*)-[YbL$_{RRRRRR}$]$^{3+}$ are small. This result is in agreement with the formation of an ion pair and the influence of the cationic complex as the paramagnetic centre.

The intensities of the two split signals of the dipicolinate ligand are equal within the accuracy of signal integration and we do not observe a measurable Pfeiffer effect, i.e. a shift of equilibrium between Λ-[Ln′(dpa)$_3$]$^{3-}$ and Δ-[Ln′(dpa)$_3$]$^{3-}$, under the influence of a chiral enantiopure partner. Similarly, the lack of CD bands reflecting f–f transition of the anionic dipicolinate complexes indicate no Pfeiffer effect caused by (*P*)-[LnL$_{RRRRRR}$]$^{3+}$.

The NMR spectra indicate that the original C_2 symmetry of (*P*)-[LnL$_{RRRRRR}$]$^{3+}$ and D_3 symmetry of [Ln′(dpa)$_3$]$^{3-}$ are effectively retained in the ion pair. This symmetry reflects dynamic exchange, where the cation and the anion are the exchanging partners between the symmetry-related binding sites. Moreover, this exchange can involve not only 1:1 association, but also 2:1, 1:2, 1:3 and various other cation/anion aggregates.[14d,21]

The DFT Calculated Structures of the (*P*)-[LnL$_{\mathrm{RRRRRR}}$]$^{3+}$/[Ln′(dpa)$_3$]$^{3-}$ Ion Pairs

Although the aggregation between (*P*)-[LnL$_{\mathrm{RRRRRR}}$]$^{3+}$ and [Ln′(dpa)$_3$]$^{3-}$ is evident in solution, we were unable to obtain crystalline salts containing these two ionic complexes. In the absence of an X-ray crystal structure we have used theoretical methods to find the mutual orientation of the cation and anion. We have assumed the simplest 1:1 pairing as the model for the interaction between the complexes. The (*P*)-[YL$_{RRRRRR}$]$^{3+}$/[Y(dpa)$_3$]$^{3-}$ pair has been chosen as a favourable starting structure for the (*P*)-[YbL$_{RRRRRR}$]$^{3+}$/[Lu(dpa)$_3$]$^{3-}$ and (*P*)-[TbL$_{RRRRRR}$]$^{3+}$/[Tb(dpa)$_3$]$^{3-}$ pairs. The structures obtained (Figure 4) indeed show tight ion pair formation with the anion bound sideways in respect to the C_2 axis of the macrocyclic complex. All calculated ion pairs form very stable systems with an interaction energy between –494 and –515 kcal/mol (Table 1), identified as minima at hyperenegy surface. Because interacting molecules have strong opposite charges we expect the electrostatic term of the interaction energy to be the most effective. For the small oppositely charged interacting systems with similar interaction energies we were unable to perform full Kitaura–Morokuma energy decomposition and show that the electrostatic term can provide over 80% of the interaction energy.[22]

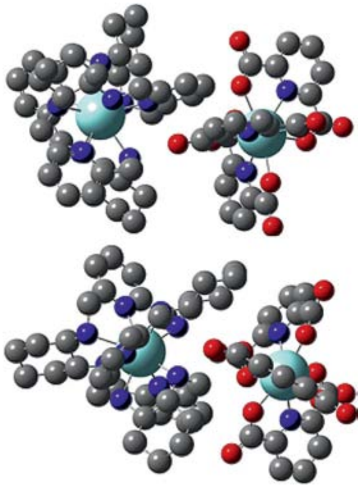

Figure 4. The calculated structure of the most stable diastereomeric ion pairs (*P*)-[YL$_{RRRRRR}$]$^{3+}$/Λ-[Y(dpa)$_3$]$^{3-}$ (top) and (*P*)-[YL$_{RRRRRR}$]$^{3+}$/Δ-[Y(dpa)$_3$]$^{3-}$ (bottom). Hydrogen atoms are not shown.

Table 1. Calculated interaction energies and Ln–Ln′ distances in the ion pairs.

Ln–Ln′	(*P*)-[LnL$_{RRRRRR}$]$^{3+}$/Λ-[Ln′(dpa)$_3$]$^{3-}$ Energy[a]	Distance[b]	(*P*)-[LnL$_{RRRRRR}$]$^{3+}$/Δ-[Ln′(dpa)$_3$]$^{3-}$ Energy[a]	Distance[b]
Y–Y	–494.33	6.992	–508.90	7.012
Tb–Tb	–511.14	7.031	–506.54	7.036
Yb–Lu	–509.90	7.002	–514.79	7.030

[a] kcal/mol. [b] Å.

The structures obtained of the 1:1 ion-pairs indicate a “docking site” on the side of the (*P*)-[LnL$_{RRRRRR}$]$^{3+}$ complex. As discussed above, the other symmetry-related docking site at the cationic complex can also be occupied by the anion because of a dynamic equilibrium or formation of a 1:2 complex. The structures of the two diastereomeric pairs (*P*)-[LnL$_{RRRRRR}$]$^{3+}$/Δ-[Ln′(dpa)$_3$]$^{3-}$ and (*P*)-[LnL$_{RRRRRR}$]$^{3+}$/Λ-[Ln′(dpa)$_3$]$^{3-}$ are not very different, although the hydrogen bond network and contacts within each pair are not the same (Figure 4). Both structures show the macrocyclic complex approaching the [Ln′(dpa)$_3$]$^{3-}$ complex roughly along the local D_3 axis of the anion. This orientation is in qualitative agreement with the NMR spectroscopic data and corresponds to the different orientation of the macrocycle and dipicolinate protons with respect to the cone aligned along the D_3 axis, determined by the $<1 - 3\cos^2\theta/r^3>$ term. Because of this orientation, the two types of protons experience dipolar shifts of opposite signs, as discussed above. We have tried to confirm experimentally the calculated structure of the ion pair by observation of NOE effects corresponding to the close contacts between the hydrogen atoms of the macrocycle and dipicolinate ligands. It should be noted that NOE NMR spectroscopy in addition to pulsed gradient spin–echo methods are often used for the investigation of ion pairs.[4,20] Unfortunately, the NOESY and ROESY spectra (Supporting Information Figure S2) indicate only close contacts within each unit, due to incomplete association.

All of the ionic pairs investigated form well defined lock–key structures. The isosurface of DFT total electron density (Supporting Information Figure S3) shows how the propeller-like anion fits into the $[LnL_{RRRRRR}]^{3+}$ cavity. Such a lock–key orientation provides very close contact between the metal ions. Despite differences in atom sizes, the distance R between the Ln^{III} ions oscillates at around 7Å (Table 1.) These close contacts are in agreement with the ^{1}H NMR spectroscopic data indicating strong interactions and the formation of a tight contact ion pair rather than the more distant solvent-separated or solvent-shared ion pair.[4] All ion pairs containing Λ isomers show a slightly shorter distance between the Ln atoms than those containing Δ isomers. In the case of a Tb/Tb complex, a shorter R distance (in the Λ isomer) is correlated with stronger interaction, however in cases of Y/Y and Yb/Lu complexes we have found the opposite correlation. Therefore, the distance between the Ln^{III} ions cannot be used as reliable quality measure of stability of such complexes. The calculated structures indicate an important role of hydrogen bonds in the formation of the (P)-$[LnL_{RRRRRR}]^{3+}/[Ln'(dpa)_3]^{3-}$ pair. The carboxylate carbonyl groups of the dipicolinate ligands as hydrogen bond acceptors, and the NH groups of the macrocycle act as hydrogen bond donors. Thus the formed (P)-$[LnL_{RRRRRR}]^{3+}/[Ln'(dpa)_3]^{3-}$ pair can be referred to more precisely as a "charge-assisted supramolecular moiety".[4a] We have found five hydrogen bonds between the cationic and anionic complex that are typical for each pair: a) a N–H···O bond, which is the strongest bond with significant shift of the proton from the cation (N–H) to the anion (O), b) a C–H···O supported N–H···O hydrogen bond, c) a bifurcated C–H···O and d) a weak C–H···O interaction (a and b are shown in the Supporting Information Figure S4). All geometrical parameters of the hydrogen bonding interactions are presented in the Supporting Information Table S1. The NBO analysis[23,24] shows charge transfer from anion to cation in each complex upon complexation. The most significant charge transfer we have observed is in the Y/Y complex pair: 0.64 and 0.25 e for the Δ and Λ diastereomers, respectively. The Tb/Tb pair transfers 0.19 and 0.23 e for the Δ and Λ diastereomers, respectively (the Yb/Lu complex pair transfers only 0.15 and 0.23 e). Inside the monomers the metal cation charges drop from +3 to +1.5 in $[Ln'(dpa)_3]^{3-}$ and +1.6 to +1.9 in $[LnL_{RRRRRR}]^{3+}$. The charge transfer between the cation and the anion is not significant, and the most dramatic rearrangement of electron density is observed inside the individual complex ions.

As indicated in Table 1, the relative energy of the two diastereomeric pairs is not very different. Single point calculations with the IEFPCM approach (solvent: water, temperature: 298.15 K, pressure: 1 atm) in the gas phase geometry yielded ΔG values for the formation of ionic pairs containing the Δ and Λ isomers equal to –51.6 and –56.9 kJ/mol, respectively. In reality, this difference is probably even smaller, which explains the lack of observation of the Pfeiffer effect.

The Interaction between the (M)-$[LnL_{RRRRRR}]^{3+}$ Diastereomers and $[Ln'(dpa)_3]^{3-}$: Pfeiffer Effect and Formation of Supramolecular Polymers

Although we did not observed any clear CD signals corresponding to the f–f transition of $[Ln'(dpa)_3]^{3-}$ induced by (P)-$[LnL_{RRRRRR}]^{3+}$ diastereomers, clear CD signals were induced by (M)-$[LnL_{RRRRRR}]^{3+}$ diastereomers (Figures 5 and 6).

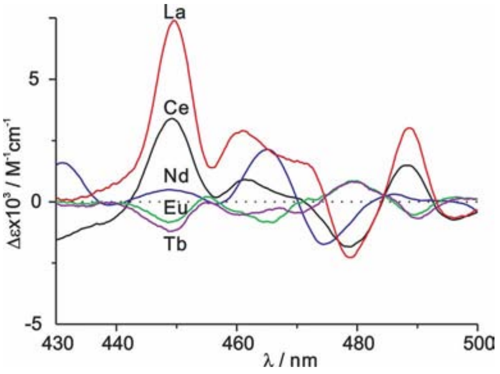

Figure 5. CD spectra of water solutions of $[Pr(dpa)_3]^{3-}$ mixed with (M)-$[LnL_{RRRRRR}]^{3+}$: (M)-$[LaL_{RRRRRR}]^{3+}$ (brown line), (M)-$[CeL_{RRRRRR}]^{3+}$ (black line), (M)-$[NdL_{RRRRRR}]^{3+}$ (blue line), (M)-$[EuL_{RRRRRR}]^{3+}$ (green line) and (M)-$[TbL_{RRRRRR}]^{3+}$ (violet line, 0.02 mM water solutions, measured 10 min after mixing the complexes).

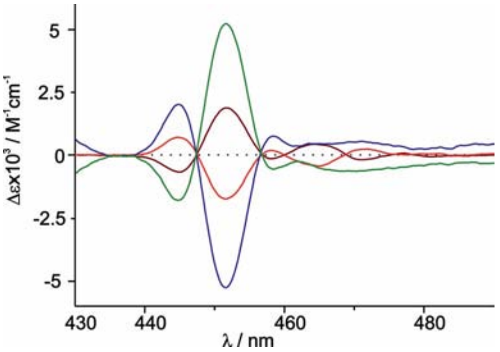

Figure 6. CD spectra of water solutions of $[Dy(dpa)_3]^{3-}$ mixed with (M)-$[LnL_{RRRRRR}]^{3+}$ or (P)-$[LnL_{SSSSSS}]^{3+}$: (M)-$[CeL_{RRRRRR}]^{3+}$ (green line), (P)-$[CeL_{SSSSSS}]^{3+}$ (blue line), (M)-$[EuL_{RRRRRR}]^{3+}$ (red line), (P)-$[EuL_{SSSSSS}]^{3+}$ (brown line, 0.02 mM water solutions, measured 10 min after mixing the complexes).

Because the $[Ln'(dpa)_3]^{3-}$ complexes, present as racemic mixtures, do not give CD signals themselves, the observed CD effects have to be caused by the interaction with the chiral enantiopure cationic complexes. As the latter (*M*)-$[LnL_{RRRRRR}]^{3+}$ complexes may also give CD spectra corresponding to f–f transitions, we tried to choose (*M*)-$[LnL_{RRRRRR}]^{3+}$/$[Ln'(dpa)_3]^{3-}$ pairs where the transitions of the Ln^{III} and Ln'^{III} ions do not overlap. For instance, we have observed CD spectra corresponding mainly to the Pr^{III} transitions in $[Pr(dpa)_3]^{3-}$ interacting with the cationic complexes (*M*)-$[LnL_{RRRRRR}]^{3+}$, where Ln^{III} = La^{III}, Ce^{III}, Nd^{III}, Eu^{III} and Tb^{III} (Figure 5). The CD spectrum observed for the mixture of (*M*)-$[LaL_{RRRRRR}]^{3+}$ with $[Pr(dpa)_3]^{3-}$ is completely different from that of (*M*)-$[PrL_{RRRRRR}]^{3+}$, so the CD f–f Pr^{III} transitions do not result from scrambling (transmetalation) of the two Ln^{III} ions, but from the disturbed equilibrium between the Δ and Λ enantiomers of the anionic Pr^{III} complex. We have also observed clear CD spectra corresponding to the Dy^{III} transitions in the $[Dy(dpa)_3]^{3-}$ complex interacting with the cationic complexes (*M*)-$[LnL_{RRRRRR}]^{3+}$, where Ln^{III} = Ce^{III} or Eu^{III} (Figure 6). The sign of the induced CD depends on the enantiomer of the cationic complex; the CD spectra obtained for the (*M*)-$[LnL_{RRRRRR}]^{3+}$/$[Ln'(dpa)_3]^{3-}$ pairs are mirror images of those obtained with the (*P*)-$[LnL_{SSSSSS}]^{3+}$/$[Ln'(dpa)_3]^{3-}$ pairs (Figure 6). This is direct evidence that the CD signals observed arise from the interactions of $[Ln'(dpa)_3]^{3-}$ with the chiral cationic complexes and the Pfeiffer effect is observed. The dynamic equilibrium between the Λ-$[Ln'(dpa)_3]^{3-}$ and Δ-$[Ln'(dpa)_3]^{3-}$ enantiomers is disturbed by the interaction with the chiral cationic complex.

A striking feature of the CD spectra of the complex mixtures is a strong dependence of the induced Cotton effect observed for the anionic dipicolinate complex on the cationic complex used. For instance a positive CD signal is observed for the 449 nm transition of the $[Pr(dpa)_3]^{3-}$ anion interacting with (*M*)-$[LnL_{RRRRRR}]^{3+}$ containing lighter Ln^{III} ions (La^{III}, Ce^{III}, Nd^{III}). In contrast, a negative CD signal is observed for the same transition of $[Pr(dpa)_3]^{3-}$ interacting with (*M*)-$[LnL_{RRRRRR}]^{3+}$ containing heavier Eu^{III} and Tb^{III} ions. Similarly, opposite signs of CD signals are observed for the f–f transitions of the Dy^{III} ion in the $[Dy(dpa)_3]^{3-}$ anion interacting with (*M*)-$[LnL_{RRRRRR}]^{3+}$ containing the lighter Ce^{III} ion in comparison with the analogous pair containing the heavier Eu^{III} ion (Figure 6). We initially attributed this effect to the transition of the (*M*)-$[LnL_{RRRRRR}]^{3+}$ complex to its (*P*)-$[LnL_{RRRRRR}]^{3+}$ diastereomer with opposite helicity. However, this process is not important in the time scale of the CD measurements as indicated by the lack of characteristic changes in the NMR and CD spectra accompanying the (*M*) to (*P*) transition.[7,8]

Closer inspection of the solutions used for the CD measurements indicated cloudiness for the (*M*)-$[LnL_{RRRRRR}]^{3+}$/$[Ln'(dpa)_3]^{3-}$ pairs containing lighter Ln^{III}. The extent of precipitate formation (decomposition) correlates roughly with the intensity of the positive 449 nm transition of the $[Pr(dpa)_3]^{3-}$ anion. Thus the CD signals observed arise from two different interactions leading to the Pfeiffer effect. The first interaction is an ion pair interaction between the intact (*M*)-$[LnL_{RRRRRR}]^{3+}$ cation and $[Ln'(dpa)_3]^{3-}$. The second interaction is between $[Ln'(dpa)_3]^{3-}$ and a decomposition product. Further clues come from NMR measurements of the solutions corresponding to the CD samples. The ^{1}H NMR spectra of the mixtures of $[Pr(dpa)_3]^{3-}$ with various (*M*)-$[LnL_{RRRRRR}]^{3+}$ complexes (Ln^{III} = La^{III}, Ce^{III}, Pr^{III}) show signals of the complex anion and cation as well as diamagnetic signals corresponding to the decomplexed macrocycle. Transmetalation between the cationic Pr^{III} complex and the anionic La^{III} and Ce^{III} complexes was not observed, i.e. the characteristic ^{1}H NMR signals of (*M*)-$[PrL_{RRRRRR}]^{3+}$ were absent. In addition to the signals of the starting complex cation and anion, characteristic signals at δ = 15.2 and 13.9 ppm were observed for all the samples. These signals correspond with $[Pr(dpa)_3]^{3-}$ interacting with some kind of decomposition product. As the signals at δ = 15.2 and 13.9 ppm do not depend on the Ln^{III} present in the cationic complex, the decomposition product has to be a demetalated derivative of macrocycle L, most likely its protonated form.

To further understand the decomposition reaction accompanying the interaction between (*M*)-$[LnL_{RRRRRR}]^{3+}$ and $[Ln'(dpa)_3]^{3-}$, and the nature of the precipitates formed, we have performed a series of a control reactions. Firstly we mixed the free macrocycle with $[Ln'(dpa)_3]^{3-}$ and did not observe any reaction. Conversely, mixing the substrates under acidic conditions, e.g. reacting the in situ generated protonated form of the macrocycle with $[Ln'(dpa)_3]^{3-}$ results in the immediate formation of precipitates. For instance the reaction of a water solution of the protonated macrocyclic amine H_3L^{3+} generated from 1 equiv. of L and three equiv. of HCl or HNO_3 with the water solution of $Na_3[Ln'(dpa)_3]\cdot nH_2O$ results in the immediate formation of precipitates. These products are practically insoluble in water and common organic solvents. Interestingly, the same reaction with $[Pr(dpa)_3]^{3-}$, monitored by ^{1}H NMR spectroscopy, is accompanied with the formation of a small amount (as judged by signal intensity) of a soluble derivative giving rise to characteristic signals at δ = 15.2 and 13.9 ppm.

The elemental analyses of the precipitates correspond to $(H_3L_{RRRRRR})[Ln'(dpa)_3]\cdot xNaNO_3\cdot yH_2O\cdot zCH_3OH$. The elemental analyses do not indicate, however, the structure of the product, in particular the possibility of the metalation of the macrocycle or formation of mixed macrocycle/dipicolinate Ln^{III} complexes. Although these precipitates gave practically no NMR spectra due to their insolubility, we were able to confirm the presence of the intact complex anion and the intact macrocycle by reacting the precipitates with a base. For instance the reaction of a suspension of $[(H_3L)\{Pr(DPA)_3\}]\cdot 2NaNO_3\cdot 10H_2O\cdot 3CH_3OH$ in D_2O/CD_3OD with three equivalents of NaOH results in complete dissolution of the precipitate and leads to a ^{1}H NMR spectrum that clearly indicates the presence of $[Pr(dpa)_3]^{3-}$ and the free macrocycle in a 1:1 ratio (Figure 7). A similar result was obtained for the Ce^{III} supramolecular polymer

(Supporting Information Figure S5). It follows that the precipitates correspond to salts of the protonated macrocycle and the intact anionic tris(dipicolinate) complexes and their reaction with bases is caused by deprotonation of the cation and formation of neutral L:

$$(H_3L_{RRRRRR})[Pr(dpa)_3]\downarrow + 3OH^- \rightarrow L + [Pr(dpa)_3]^{3-} + 3H_2O$$

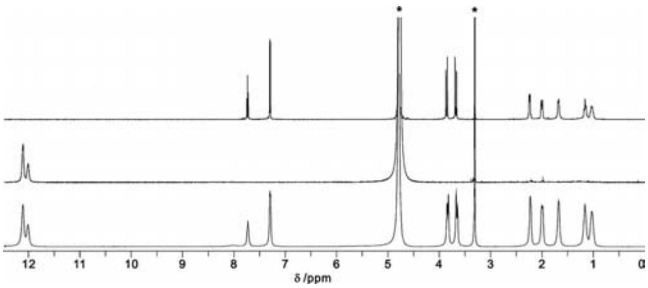

Figure 7. ^1H NMR spectra (D_2O/CD_3OD, 1:1 v/v solutions) of L (top), the $[Pr(dpa)_3]^{3-}$ complex (middle) and the $(H_3L_{RRRRRR})^{3+}/[Pr(dpa)_3]^{3-}$ supramolecular polymer reacted with 3 equiv. of NaOH (bottom).

Interestingly, the same kind of $(H_3L_{RRRRRR})[Pr(dpa)_3]$ precipitates are formed in the reaction of macrocyclic complexes with dipicolinic acid, which is represented by the simplified reaction:

$$(M)\text{-}[LnL_{RRRRRR}]^{3+} + 3H_2dpa \rightarrow (H_3L_{RRRRRR})[Ln(dpa)_3]\downarrow + 3H^+$$

The reaction reflects the competition for the Ln^{III} ion between the macrocyclic and chelating ligand and its equilibrium is influenced by the formation of an insoluble product containing the chelate complex. This reaction is particularly easy for the complexes of La^{III} and Ce^{III} where immediate formation of precipitate is observed. On the other hand, the more stable diastereomeric complexes (*P*)-$[LnL_{RRRRRR}]^{3+}$ of Lu^{III} and Yb^{III} do not form precipitates with dipicolinic acid in water solutions even after several days.

The $(H_3L_{RRRRRR})[Ln'(dpa)_3]$ precipitates are amorphous and we were not able to obtain crystals for X-ray structure determination. The highly insoluble nature of these compounds suggests that they are polymeric species rather than simple ionic salts. In particular, a supramolecular linear polymer resulting from organization of the D_3 symmetric $[Ln'(dpa)_3]^{3-}$ propellers along the C_3 axis of protonated macrocycles $(H_3L_{RRRRRR})^{3+}$, maximizing the hydrogen bond interactions and forming tight anion–cation contacts is a particularly appealing possibility. A model of the proposed linear polymer is presented in Figure 8.

Presumably the cloudiness of some of the complex mixtures used for CD measurements is due to the formation of insoluble products of the type $(H_3L_{RRRRRR})[Ln'(dpa)_3]$. The protonated form of the macrocycle was formed by slow dissociation of the macrocyclic complex followed by hydrolysis. Possibly, before the insoluble polymeric products precipitate, some sort of ion pair, with a given anion to cation ratio and given protonation state of the macrocycle, is formed, which is soluble enough to give a CD spectrum. Likely this transient form of the ion pair is related to the ^1H NMR signals at $\delta = 15.2$ and 13.9 ppm in the case of the $[Pr(dpa)_3]^{3-}$ derivative. This hypothesis explains the strong variation of the induced CD signals of $[Ln'(dpa)_3]^{3-}$ with the change of Ln^{III} in the series of the interacting (*M*)-$[LnL_{RRRRRR}]^{3+}$ cationic complexes. Firstly, the different shape of the protonated macrocyclic cation[25] $(H_3L_{RRRRRR})^{3+}$ in comparison with the shape of the complex cations (*M*)-$[LnL_{RRRRRR}]^{3+}$ results in the different preference for the Λ-$[Ln'(dpa)_3]^{3-}$ or Δ-$[Ln'(dpa)_3]^{3-}$ enantiomers of the anionic complex, hence the opposite Pfeiffer effect. Secondly, the stability of the (*M*)-$[LnL_{RRRRRR}]^{3+}$ complexes differs along the series of the Ln^{III} ions. The larger ions such as La^{III} and Ce^{III} form less stable complexes that dissociate more easily and undergo hydrolysis, hence the Pfeiffer effect observed for the corresponding mixtures is predominantly due to the interaction of $[Ln'(dpa)_3]^{3-}$ with some form of the protonated macrocycle. On the other hand the smaller Ln^{III} ions, such as Tb^{III}, form more stable (*M*)-$[LnL_{RRRRRR}]^{3+}$ complexes and the Pfeiffer effect is caused predominantly by the interaction of $[Ln'(dpa)_3]^{3-}$ with the intact complex cation. Finally for complexes such as (*M*)-$[NdL_{RRRRRR}]^{3+}$ both types of cation are present and the corresponding Pfeiffer effects are largely cancelled.

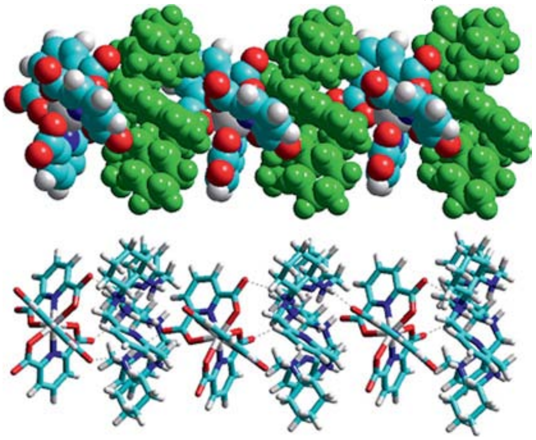

Figure 8. The MM+ model structure of the $(H_3L_{RRRRRR})^{3+}/[Ln'(dpa)_3]^{3-}$ supramolecular polymer (the protonated macrocycle L in green).

Conclusions

The (*M*)-$[LnL_{RRRRRR}]^{3+}$ diastereomers of the cationic macrocyclic complexes form tight ion pairs with anionic Ln'^{III} tris(dipicolinate) complexes indicated by the strong paramagnetic shift experienced by the signals of a diamagnetic cation interacting with paramagnetic anions. This ion pair interaction leads to spectral enantiodifferentiation of the Λ-$[Ln'(dpa)_3]^{3-}$ and Δ-$[Ln'(dpa)_3]^{3-}$ enantiomers of the anionic complex, which is seen by a doubling of the dipicolinate ^1H NMR signals. On the other hand, no Pfeiffer effect was observed with these diastereomers of the cationic complex, thus indicating no substantial preference of the complex cation for either the Λ or Δ enantiomer of the complex anion. DFT calculations indicate the formation of stable

(*M*)-$[\mathrm{LnL}_{RRRRRR}]^{3+}$/$[\mathrm{Ln'(dpa)_3}]^{3-}$ pairs (with $\Delta E \approx 500$ kcal/mol). The calculated structures show ion pairing assisted by the formation of hydrogen bonds between the complex cation and the complex anion.

The mixtures of (*M*)-$[\mathrm{LnL}_{RRRRRR}]^{3+}$ diastereomers of the cationic complexes and the anionic complexes $[\mathrm{Ln'(dpa)_3}]^{3-}$ give rise to CD spectra corresponding to the f–f transitions of the anionic complex. These spectra indicate a Pfeiffer effect, which is a shift of equilibrium between the Λ-$[\mathrm{Ln'(dpa)_3}]^{3-}$ and Δ-$[\mathrm{Ln'(dpa)_3}]^{3-}$ enantiomers. Closer analysis indicates that this effect arises from two kinds of interactions. The first is ion pair formation between the anionic complex and the intact cationic complex. The second is most likely an ion pair formation between the complex anion and some form of the protonated macrocycle.

The protonated macrocycle $(\mathrm{H_3L}_{RRRRRR})^{3+}$ forms highly insoluble salts with $[\mathrm{Ln'(dpa)_3}]^{3-}$. We propose that these compounds are supramolecular linear polymers in which the cationic protonated macrocycle interacts with the tris(dipicolinate) Ln′$^{\mathrm{III}}$ complexes through ion pairing and multiple hydrogen bonds. These supramolecular compounds are formed in the reaction of the macrocycle L, acids and $[\mathrm{Ln'(dpa)_3}]^{3-}$ anions. The same product can be also formed in the reaction of the complex cations (*M*)-$[\mathrm{LnL}_{RRRRRR}]^{3+}$ with three equivalents of dipicolinic acid. To the best of our knowledge this is the first example of a reaction of a chelate ligand with a macrocyclic complex resulting in formation of a supramolecular assembly between the formed chelate complex and protonated macrocycle.

Experimental and Computational Section

Methods: The NMR spectra were measured with Bruker Avance 500 and AMX 300 spectrometers. The CD spectra were measured with a Jasco J-715 Spectropolarimeter. The elemental analyses were carried out with a Perkin–Elmer 2400 CHN elemental analyzer. The DFT theory that has become a standard computation level for molecular complexes is also useful to investigate ion-pairing.[26] We have chosen DFT level theory with the hybrid functional of Truhlar and Zhao M062X[27] with split valance effective core potential effective for the lanthanides by Stevens, Basch and Krauss (CEP-31G).[28–30] All calculations have been performed with Gaussian 09[31] computer code. The model of the supramolecular polymer was generated using the HyperChem program.[32]

Synthesis: The cationic (*P*)-$[\mathrm{LnL}_{RRRRRR}](\mathrm{NO_3})_3$ and (*M*)-$[\mathrm{LnL}_{RRRRRR}](\mathrm{NO_3})_3$ complexes were synthesized as described previously.[7,8] The anionic Ln$^{\mathrm{III}}$ trisdipicolinate complexes $[\mathrm{Na_3Ln'(dpa)_3}]\cdot n\mathrm{H_2O}$ were synthesized using modified literature procedure.[9a–9c]

Preparation of the $(\mathrm{H_3L})[\{\mathrm{Ln'(dpa)_3}\}]$ supramolecular polymers:

Method A: $[\mathrm{Na_3Ln(DPA)_3}]\cdot n\mathrm{H_2O}$ (0.1 mmol) was dissolved in water (5 mL) and combined with a solution of of L_{RRRRRR} (0.1 mmol) in MeOH (5 mL). Aqueous $\mathrm{HNO_3}$ solution (1.5 mL, 3 mmol, 2 M) was added and the mixture was stirred for 1 day. The precipitate was collected by filtration, washed with water/MeOH (1 mL) and dried in vacuo.

$(\mathrm{H_3L})[\{\mathrm{Ce(dpa)_3}\}]\cdot 2\mathrm{NaNO_3}\cdot 4\mathrm{H_2O}\cdot 8\mathrm{CH_3OH}$: Yield 117 mg (65.4 %). $[(\mathrm{C_{39}H_{60}N_9})(\mathrm{C_{21}H_9N_3O_{12}Ce})](\mathrm{NaNO_3})_2(\mathrm{H_2O})_4(\mathrm{CH_3OH})_8$ (1788.79): calcd. C 45.66, H 6.14, N 10.96; found C 45.62, H 6.14, N 11.22.

$(\mathrm{H_3L})[\{\mathrm{Pr(dpa)_3}\}]\cdot 2\mathrm{NaNO_3}\cdot 10\mathrm{H_2O}\cdot 3\mathrm{CH_3OH}$: Yield 117 mg (67.3 %). $[(\mathrm{C_{39}H_{60}N_9})(\mathrm{C_{21}H_9N_3O_{12}Pr})](\mathrm{NaNO_3})_2(\mathrm{H_2O})_{10}(\mathrm{CH_3OH})_3$ (1737.46): calcd. C 43.55, H 5.86, N 11.29; found C 43.50, H 5.92, N 10.99.

$(\mathrm{H_3L})[\{\mathrm{Dy(dpa)_3}\}]\cdot 3\mathrm{NaNO_3}\cdot 4\mathrm{H_2O}\cdot 12\mathrm{CH_3OH}$: Yield 130 mg (64.2 %). $[(\mathrm{C_{39}H_{60}N_9})(\mathrm{C_{21}H_9N_3O_{12}Dy})](\mathrm{NaNO_3})_3(\mathrm{H_2O})_4(\mathrm{CH_3OH})_{12}$ (2024.33): calcd. C 42.72, H 6.22, N 10.38; found C 42.80, H 5.97, N 10.04.

$(\mathrm{H_3L})[\{\mathrm{Yb(dpa)_3}\}]\cdot 3\mathrm{NaNO_3}\cdot 4\mathrm{H_2O}\cdot 9\mathrm{CH_3OH}$: Yield 106 mg (54.7 %). $[(\mathrm{C_{39}H_{60}N_9})(\mathrm{C_{21}H_9N_3O_{12}Yb})](\mathrm{NaNO_3})_3(\mathrm{H_2O})_4(\mathrm{CH_3OH})_9$ (1938.75): calcd. C 42.75, H 5.87, N 10.84; found C 42.76, H 5.67, N 10.51.

$(\mathrm{H_3L})[\{\mathrm{Lu(dpa)_3}\}]\cdot 3\mathrm{NaNO_3}\cdot 8\mathrm{H_2O}\cdot 6\mathrm{CH_3OH}$: Yield 122 mg (62.1 %). $[(\mathrm{C_{39}H_{60}N_9})(\mathrm{C_{21}H_9N_3O_{12}Lu})](\mathrm{NaNO_3})_3(\mathrm{H_2O})_8(\mathrm{CH_3OH})_6$ (1916.61): calcd. C 41.36, H 5.73, N 10.96; found C 41.33, H 5.74, N 10.91.

Method B: (*M*)-$[\mathrm{Pr}(\mathrm{L}_{RRRRRR})](\mathrm{NO_3})_3\cdot(\mathrm{H_2O})$ (99.7 mg, 0.1 mmol) was dissolved in MeOH (5 mL) and combined with a solution of $\mathrm{H_2DPA}$ (50.2 mg, 0.3 mmol) in water (5 mL). After 10 min the resulting solution became cloudy. The mixture was stirred for 1 day to complete reaction. The precipitate was collected by filtration, washed with MeOH/water (1:1, 1 mL) and dried in vacuo.

$(\mathrm{H_3L})[\{\mathrm{Pr(dpa)_3}\}]\cdot 3\mathrm{HNO_3}\cdot 12\mathrm{H_2O}\cdot 2\mathrm{CH_3OH}$: Yield 122 mg (69.1 %). $[(\mathrm{C_{39}H_{60}N_9})(\mathrm{C_{21}H_9N_3O_{12}Pr})](\mathrm{HNO_3})_3(\mathrm{H_2O})_{12}(\mathrm{CH_3OH})_2$ (1760.49): calcd. C 42.30, H 5.95, N 11.93; found C 42.11, H 5.69, N 11.62.

Supporting Information (see footnote on the first page of this article): Figures S1–S4, Table S1 (NMR spectra and views of the calculated structures, and parameters for the hydrogen bonds are presented as well as the coordinates (pdb format) of fully optimized: (*P*)-$[\mathrm{YL}_{RRRRRR}]^{3+}$/Δ-$[\mathrm{Y(dpa)_3}]^{3-}$, (*P*)-$[\mathrm{YL}_{RRRRRR}]^{3+}$/Λ-$[\mathrm{Y(dpa)_3}]^{3-}$, (*P*)-$[\mathrm{TbL}_{RRRRRR}]^{3+}$/Δ-$[\mathrm{Tb(dpa)_3}]^{3-}$, (*P*)-$[\mathrm{TbL}_{\mathrm{RRRRRR}}]^{3+}$/Λ-$[\mathrm{Tb(dpa)_3}]^{3-}$, (*P*)-$[\mathrm{LuL}_{RRRRRR}]^{3+}$/Δ-$[\mathrm{Yb(dpa)_3}]^{3-}$ and (*P*)-$[\mathrm{LuL}_{RRRRRR}]^{3+}$ /Λ-$[\mathrm{Yb(dpa)_3}]^{3-}$.

Acknowledgments

This work was supported by the Polish Ministry of Science and Higher Education (grant MNiSW N N204 017135). The computational section has been supported by the Wroclaw Centre of Networking and Supercomputing.

---

[1] a) A. Macchioni, *Chem. Rev.* **2005**, *105*, 2039–2073; b) Y. Marcus, G. Hefter, *Chem. Rev.* **2006**, *106*, 4585–4621; c) B. Hess, N. F. A. van der Vegt, *Proc. Natl. Acad. Sci. USA* **2009**, *106*, 13296–13300; d) Y. J. Zhang, P. S. Cremer, *Curr. Opin. Chem. Biol.* **2006**, *10*, 658–663.

[2] J. Ren, C. S. Springer Jr., A. D. Sherry, *Inorg. Chem.* **1997**, *36*, 3493–3498.

[3] D. M. Corsi, H. van Bekkum, J. Peters, *Inorg. Chem.* **2000**, *39*, 4802–4808.

[4] a) J. Lacour, D. Moraleda, *Chem. Commun.* **2009**, 7073–7089; b) H. Amouri, M. Gruselle, in: *Chirality in Transition Metal Chemistry: Molecules, Supramolecular Assemblies and Materials* Wiley Chichester, UK, **2008**, chapter 4; c) I. Correia, H. Amouri, C. Cordier, *Organometallics* **2007**, *26*, 1150–1156; d) S. D. Bergman, R. Frantz, D. Gut, M. Kol, J. Lacour, *Chem. Commun.* **2006**, 850–852; e) R. Frantz, A. Pinto, S. Constant, G. Bernardinelli, J. Lacour, *Angew. Chem.* **2005**, *117*, 5188; *An-*

gew. Chem. Int. Ed. **2005**, *44*, 5060–5064; f) L. Mimassi, C. Guyard-Duhayon, M. M. Rager, H. Amouri, *Inorg. Chem.* **2004**, *43*, 6644–6649; g) R. Caspar, H. Amouri, M. Gruselle, C. Cordier, B. Malezieux, R. Duval, H. Leveque, *Eur. J. Inorg. Chem.* **2003**, 499–505; h) M. Gruselle, R. Thouvenot, R. Caspar, K. Boubekeur, H. Amouri, M. Ivanov, K. Tonsuaadu, *Mendeleev Commun.* **2004**, *14*, 282–283; i) L. Mimassi, C. Cordier, C. Guyard-Duhayon, B. E. Mann, H. Amouri, *Organometallics* **2007**, *26*, 860–864; j) , H. Amouri, R. Caspar, M. Gruselle, C. Guyard-Duhayon, K. Boubekeur, D. A. Lev, L. S. B. Collins, D. B. Grotjahn, *Organometallics* **2004**, *23*, 4338–4341.

[5] D. Uraguchi, T. Ito, T. Ooi, *J. Am. Chem. Soc.* **2009**, *131*, 3836–3837.

[6] a) D. Rix, J. Lacour, *Angew. Chem.* **2010**, *122*, 2; *Angew. Chem. Int. Ed.* **2010**, *49*, 2–5; b) D. Uraguchi, Y. Ueki, T. Ooi, *Science* **2009**, *326*, 120–123.

[7] J. Gregoliński, J. Lisowski, *Angew. Chem.* **2006**, *118*, 6268; *Angew. Chem. Int. Ed.* **2006**, *45*, 6122–6126.

[8] J. Gregolinski, P. Starynowicz, K. T. Hua, J. L. Lunkley, G. Muller, J. Lisowski, *J. Am. Chem. Soc.* **2008**, *130*, 17761–17773.

[9] a) J. Albertsson, *Acta Chem. Scand.* **1970**, *24*, 1213; b) J. Albertsson, *Acta Chem. Scand.* **1972**, *26*, 985; c) P. A. Brayshaw, J.-C. G. Bünzli, P. Froidevaux, J. M. Harrowfield, Y. Kim, A. N. Sobolev, *Inorg. Chem.* **1995**, *34*, 2068; d) N. Ouali, B. Bocquet, S. Rigault, P.-Y. Morgantini, J. Weber, C. Piguet, *Inorg. Chem.* **2002**, *41*, 1436–1445; P. Gawryszewska, J. Legendziewicz, Z. Ciunik, N. Esfandiari, G. Muller, C. Piguet, M. Cantuel, J. P. Riehl, *Chirality* **2006**, *18*, 406–412.

[10] a) G. Muller, *Dalton Trans.* **2009**, 9692–9707; b) G. Muller, F. C. Muller, C. L. Maupin, J. P. Riehl, *Chem. Commun.* **2005**, 3615–3617.

[11] X.-C. Su, H. Liang, K. V. Loscha, G. Otting, *J. Am. Chem. Soc.* **2009**, *131*, 10352–10353.

[12] N. Tancrez, C. Feuvrie, I. Ledoux, J. Zyss, L. Toupet, H. Le Bozec, O. Maury, *J. Am. Chem. Soc.* **2005**, *127*, 13474–13475.

[13] G. Pompidor, A. D'Aleo, J. Vicat, L. Toupet, N. Giraud, R. Kahn, O. Maury, *Angew. Chem.* **2008**, *120*, 3436; *Angew. Chem. Int. Ed.* **2008**, *47*, 3388–3391.

[14] a) P. Pfeiffer, K. Quehl, *Ber. Dtsch. Chem. Ges.* **1931**, *64*, 2667; b) P. Pfeiffer, K. Quehl, *Ber. Dtsch. Chem. Ges.* **1932**, *65*, 560; c) P. Pfeiffer, Y. Nakasuka, *Ber. Dtsch. Chem. Ges.* **1933**, *66*, 410; d) P. E. Schipper, *J. Am. Chem. Soc.* **1978**, *100*, 1079–1084.

[15] a) A. Moussa, C. Pham, S. Bommireddy, G. Muller, *Chirality* **2009**, *21*, 497–506; b) R. A. Hopkins, D. H. Metcalf, F. S. Richardson, *Chirality* **2008**, *20*, 511–523; c) S. C. J. Meskers, M. Ubbink, G. W. Canters, H. P. J. M. Dekkers, *J. Phys. Chem.* **1996**, *100*, 17957–17969; d) E. Huskowska, J. P. Riehl, *Inorg. Chem.* **1995**, *34*, 5615–5621; e) D. H. Metcaf, S. W. Snyder, J. N. Demas, F. S. Richardson, *J. Am. Chem. Soc.* **1990**, *112*, 469–479; f) D. H. Metcaf, S. W. Snyder, J. N. Demas, F. S. Richardson, *J. Am. Chem. Soc.* **1990**, *112*, 5681–5695; g) N. Coruh, G. L. Hilmes, J. P. Riehl, *Inorg. Chem.* **1988**, *27*, 3647–3651.

[16] a) T. N. Parac-Vogt, K. Binnemans, C. Görller-Walrand, *ChemPhysChem* **2001**, *2*, 767–769; b) T. N. Parac-Vogt, K. Binnemans, C. Görller-Walrand, *J. Chem. Soc., Dalton Trans.* **2002**, 1602–1606.

[17] a) M. P. Placidi, A. J. L. Villaraza, L. S. Natrajan, D. Sykes, A. M. Kenwright, S. Faulkner, *J. Am. Chem. Soc.* **2009**, *131*, 9916–9917; b) S. Tamburini, S. Sitran, V. Peruzzo, P. A. Vigato, *Eur. J. Inorg. Chem.* **2009**, 155–167; c) X.-Y. Chen, Y. Bretonniere, J. Pecaut, D. Imbert, J.-C. G. Bünzli, M. Mazzanti, *Inorg. Chem.* **2007**, *46*, 625–637; d) J.-P. Costes, F. Dahan, F. Nicodeme, *Inorg. Chem.* **2003**, *42*, 6556–6563.

[18] For NMR of paramagnetic complexes see: a) G. N. La Mar, W. DeW. Horrocks Jr., R. H. Holm (Eds.), *NMR of Paramagnetic Molecules*, Academic Press, New York, **1973**; b) I. Bertini, C. Luchinat, *NMR of Paramagnetic Molecules in Biological Systems*, Benjamin/Cummings, Menlo Park, CA, **1986**; c) I. Bertini, P. Turano, A. J. Vila, *Chem. Rev.* **1993**, *93*, 2833; d) I. Bertini, C. Luchinat, *Coord. Chem. Rev.* **1996**, 150, 1; e) A. D. Sherry, C. F. G. C.Geraldes, in: *Lanthanide Probes in Life, Chemical and Earth Sciences. Theory and Practice* (Eds.: J.-C. G. Bünzli, G. R. Choppin), Elsevier, Amsterdam, **1989**, chapter 4; J. A. Peters, J. Huskens, D. J. Raber, *J. Prog. NMR Spectrosc.* **1996**, *28*, 283.

[19] a) B. Bleaney, *J. Magn. Reson.* **1972**, *8*, *91*; b) B. Bleaney, C. M. Dobson, B. A. Levine, R. B. Martin, R. J. P. Williams, A. V. J. Xavier, *J. Chem. Soc., Chem. Commun.* **1972**, 791.

[20] a) A. Macchioni, A. Magistrato, I. Orabona, F. Ruffo, U. Rothlisberger, C. Zuccaccia, *New J. Chem.* **2003**, *27*, 455–458; b) D. Zuccaccia, G. Bellachioma, G. Cardaci, G. Ciancaleoni, C. Zuccaccia, E. Clot, A. Macchioni, *Organometallics* **2007**, *26*, 3930–3946; c) P. S. Pregosin, P. G. A. Kumar, I. Fernandez, *Chem. Rev.* **2005**, *105*, 2977–2998; d) A. Macchioni, *Eur. J. Inorg. Chem.* **2003**, 195–205.

[21] D. Zuccaccia, E. Foresti, S. Pettirossi, P. Sabatino, C. Zuccaccia, A. Macchioni, *Organometallics* **2007**, *26*, 6099–6105.

[22] E. Gumienna-Kontecka, G. Berthon, I. O. Fritsky, R. Wieczorek, Z. Latajka, H. Kozlowski, *J. Chem. Soc., Dalton Trans.* **2000**, *22*, 4201–4208.

[23] J. P. Foster, F. Weinhold, *J. Am. Chem. Soc.* **1980**, *102*, 7211–7218.

[24] A. E. Reed, F. Weinhold, *J. Chem. Phys.* **1983**, *78*, 4066–4073.

[25] A. Gonzalez-Alvarez, I. Alfonso, F. Lopez-Oritz, A. Aguirre, S. Garcia-Granda, V. Gotor, *Eur. J. Org. Chem.* **2004**, 1117–1127.

[26] E. Clot, *Eur. J. Inorg. Chem.* **2009**, 2319–2328.

[27] Y. Zhao, D. G. Truhlar, *Theor. Chem. Acc.* **2008**, *120*, 215–41.

[28] W. J. Stevens, H. Basch, M. Krauss, *J. Chem. Phys.* **1984**, *81*, 6026–6033.

[29] W. J. Stevens, M. Krauss, H. Basch, P. G. Jasien, *Can. J. Chem.* **1992**, *70*, 612–630.

[30] T. R. Cundari, W. J. Stevens, *J. Chem. Phys.* **1993**, *98*, 5555–5565.

[31] M. J. Frisch, G. W. Trucks, H. B. Schlegel, G. E. Scuseria, M. A. Robb, J. R. Cheeseman, J. A. Montgomery Jr., T. Vreven, K. N. Kudin, J. C. Burant, J. M. Millam, S. S. Iyengar, J. Tomasi, V. Barone, B. Mennucci, M. Cossi, G. Scalmani, N. Rega, G. A. Petersson, H. Nakatsuji, M. Hada, M. Ehara, K. Toyota, R. Fukuda, J. Hasegawa, M. Ishida, T. Nakajima, Y. Honda, O. Kitao, H. Nakai, M. Klene, X. Li, J. E. Knox, H. P. Hratchian, J. B. Cross, V. Bakken, C. Adamo, J. Jaramillo, R. Gomperts, R. E. Stratmann, O. Yazyev, A. J. Austin, R. Cammi, C. Pomelli, J. W. Ochterski, P. Y. Ayala, K. Morokuma, G. A. Voth, P. Salvador, J. J. Dannenberg, V. G. Zakrzewski, S. Dapprich, A. D. Daniels, M. C. Strain, O. Farkas, D. K. Malick, A. D. Rabuck, K. Raghavachari, J. B. Foresman, J. V. Ortiz, Q. Cui, A. G. Baboul, S. Clifford, J. Cioslowski, B. B. Stefanov, G. Liu, A. Liashenko, P. Piskorz, I. Komaromi, R. L. Martin, D. J. Fox, T. Keith, M. A. Al-Laham, C. Y. Peng, A. Nanayakkara, M. Challacombe, P. M. W. Gill, B. Johnson, W. Chen, M. W. Wong, C. Gonzalez, J. A. Pople, *Gaussian 09*, revision A.02, Gaussian, Inc., Wallingford CT, **2004**.

[32] *HyperChem*, for Windows®, release 7.0, Hypercube, Inc.

Received: February 10, 2011